

Image Fusion via Vision-Language Model

Zixiang Zhao^{1,2} Lilun Deng¹ Haowen Bai¹ Yukun Cui¹ Zhipeng Zhang^{2,3} Yulun Zhang²
Haotong Qin² Dongdong Chen⁴ Jiangshe Zhang¹ Peng Wang³ Luc Van Gool²

¹ Xi'an Jiaotong University ² Computer Vision Lab, ETH Zürich
³ Northwestern Polytechnical University ⁴ Heriot-Watt University

Abstract

Image fusion integrates essential information from multiple source images into a single composite, emphasizing the highlighting structure and textures, and refining imperfect areas. Existing methods predominantly focus on pixel-level and semantic visual features for recognition. However, they insufficiently explore the deeper semantic information at a text-level beyond vision. Therefore, we introduce a novel fusion paradigm named image Fusion via Vision-Language Model (FILM), for the first time, utilizing explicit textual information in different source images to guide image fusion. In FILM, input images are firstly processed to generate semantic prompts, which are then fed into ChatGPT to obtain rich textual descriptions. These descriptions are fused in the textual domain and guide the extraction of crucial visual features from the source images through cross-attention, resulting in a deeper level of contextual understanding directed by textual semantic information. The final fused image is created by vision feature decoder. This paradigm achieves satisfactory results in four image fusion tasks: infrared-visible, medical, multi-exposure, and multi-focus image fusion. We also propose a vision-language dataset containing ChatGPT-based paragraph descriptions for the eight image fusion datasets in four fusion tasks, facilitating future research in vision-language model-based image fusion. Code and dataset will be released.

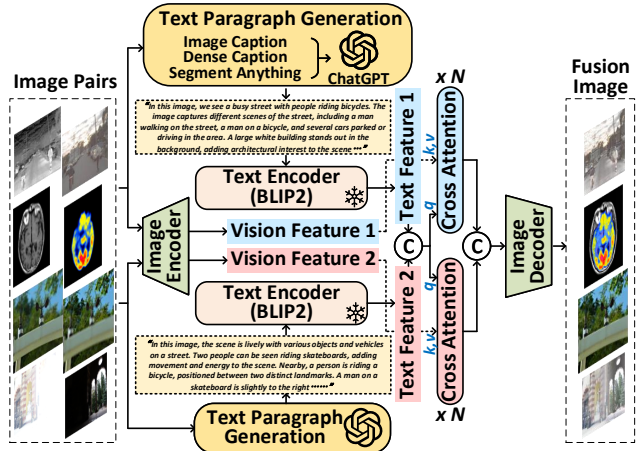


Figure 1. Workflow for our FILM. Input images are first processed to create prompts for the ChatGPT model, which then generate detailed textual descriptions. These descriptions help to get fused textual features via the frozen BLIP2 [20] model. Then, these textual features are fused and guide the extraction and fusion of visual features via cross-attention, enhancing contextual understanding with text-based semantic information. Finally, the fusion image is output by the image decoder.

1. Introduction

Image fusion [24, 72, 80, 82], standing as a critical technique in computer vision, combines information from multiple source images to create a single image that is more informative and suitable for human or machine perception. The realm of image fusion encompasses several sub-tasks, each addressing unique challenges and applications. Representatively, infrared-visible image fusion combines infrared and visible images, enhancing object representation under varied illumination conditions [80, 82]. Medical image fu-

sion integrates different modalities of clinical images such as MRI and CT scans, offering a more comprehensive view for diagnosis and treatment planning [12, 21, 56]. Multi-exposure image fusion merges images taken with different exposure settings to capture a wider range of luminance, which is crucial in high dynamic range imaging [32, 33]. Lastly, multi-focus image fusion merges images focused on different planes to produce a uniformly sharp image, invaluable in microscopy and macro photography [4, 72].

Despite its widespread application, the current state of image fusion is marred by a notable limitation: an over-reliance on visual features. The prevalent methodologies in this field predominantly center around the vision feature extraction, alignment, fusion, and reconstruction, prioritizing aspects like texture, contrast, highlight information and pixel registration [23, 80]. This consequently neglects the

deeper, semantic layers of information that images inherently possess. Approaches that integrate downstream pattern recognition tasks like semantic segmentation [26, 44, 45] and object detection [24, 43, 76], although progressive, still fall short as they remain concentrate on the superficial semantics derived from visual pixel level cues rather than the deeper, more nuanced textual information that images can convey. Therefore, how to better utilize the deeper-semantic features that go beyond visual information in images, becomes a breakthrough point that urgently needs to be addressed.

With the development of large language models [37], some work attempts [36, 40, 70, 83] to perform Vision Language Model (VLM) Fusion and Alignment as supplementary. These models, which include notable architectures like CLIP [40] and GPT4 [36], demonstrate remarkable proficiency in understanding and generating content that synergizes visual and textual components. They not only tap into the knowledge capabilities of the large language model, but also align and fuse with visual information. This synergy has the potential to significantly enhance image fusion processes, offering a pathway to incorporate deeper semantic understanding guided by language, thereby enabling a more comprehensive and contextually rich fusion process. For instance, when describing two multi-modal images from the same scene, the descriptions should focus on the response characteristics unique to each modality; for descriptions of multi-focus images, the text should pay greater attention to the areas of perfect imaging that align with their focal points. Thus, we can extract textual descriptions from images based on large vision-language model and, after integrating descriptions on the textual feature level, we then use fused text features to guide the extraction and fusion of features at the image and vision level.

Therefore, in this paper, we propose a novel algorithm called *Image Fusion via Vision-Language Model (FILM)*. This approach integrates the capabilities of VLMs into the image fusion process for the first time, leveraging the semantic understanding derived from textual data to guide and enhance the fusion of visual features. Our methodology comprises three components: text feature fusion, language-guided vision feature fusion, and vision feature decoder. The workflow of these components is depicted in Fig. 1. Our contributions are summarized as follows:

- We propose a novel paradigm for image fusion. To our knowledge, this is the first instance of incorporating explicit (*language model derived*) textual guidance into image fusion algorithms. This approach aids in the deeper understanding of text-level semantic information, facilitating the extraction and fusion of strengths from each source image.
- Our model has achieved satisfactory results in infrared-visible, medical, multi-exposure, and multi-focus image fusion tasks, demonstrating its effectiveness across various

application scenarios.

- We introduce a series of vision-language benchmark datasets for image fusion covering eight fashion datasets across four fusion tasks. These datasets comprise manually refined prompts tailored for the ChatGPT model, alongside paired textual descriptions generated by ChatGPT, which are designed to facilitate subsequent research in image fusion using vision-language models.

2. Related Work

In this section, we will review the image fusion algorithms in the era of deep learning (DL) and introduce the key technology used in our paper: the Vision-Language Model (VLM).

DL-based Image fusion. In the era of deep learning, neural networks are often used for source feature extraction, feature fusion, and fused image reconstruction [72, 80]. **(a)** In *multi-modal image fusion*, since there is no ground truth available, it inherently belongs to an unsupervised task. The fusion methods can be divided into generative and discriminative categories [73]. Generative algorithms model the latent space manifold through generative adversarial network (GAN) [24, 31] or denoising diffusion models [82], making the distribution gap between the source and fused images as close as possible. On the other hand, discriminative models, based on regression ideas, use the model-driven [18, 64, 78, 79] or data-driven [17, 77, 80] auto-encoder structures to learn the source-fusion images mapping. Additionally, downstream cross-modal pattern recognition tasks, such as object detection [24, 43, 76] and semantic segmentation [26, 44, 45], are employed to make the fused images highlight features and regions containing vision-based semantic information [76]. **(b)** In *digital image fusion*, supervised fusion algorithms often obtain a mapping from imperfect source images to perfect ground truth by predicting decision maps or reconstructing images [4, 28, 29, 54, 55, 66]. For issues where perfect training ground truth, like normally-exposed and all-focus images, are hard to obtain, unsupervised algorithms often reconstruct fused images based on CNN [1, 5, 6, 8, 10, 38], Transformer [8, 39] or GAN [3, 9, 58, 65]. The feature substitution or fusion, with the help of no-reference quality metrics [27, 63], usually occurrence in image domains, frequency domains, or feature spaces [29, 51, 52]. **(c)** Furthermore, registration-based methods focus on solving the misalignment issue in multi-source image inputs, reducing artifacts in the fused images [13, 49, 60]. Meanwhile, unified frameworks explore the meta-information in different fusion tasks, investigating the mutual promotion effects and alleviating the issues of lacking paired training data and absence of ground truth [23, 59].

Vision-Language model. Recently, visual language multimodal learning [2, 19, 40, 62] has become a hot research topic. In particular, vision-language model (VLM)

[19, 36, 50, 70, 83] such as BLIP [19, 20], DALL-E [41, 42], and GPT4 [36] show powerful performance in several downstream tasks. BLIP demonstrates powerful knowledge prompt capabilities in bridging between frozen visual feature pre-trained encoders and frozen large language models. GPT4 also shows strong general performance based on visual language pre-training. With the help of these large models [36, 48], a lot of studies [70, 83] in the field of image captioning have turned into guiding the large models to describe images in detail in the form of natural language. These large models provide external common knowledge for image caption. The key details information from the image such as dense caption, can provide a strong explicit prompt. It allows the image to be presented in a descriptive form that covers the key information. Inspired by this, we aim to introduce a vision-language model to image fusion so that text can guide image fusion in an effective and intuitive way. **Comparison with existing approaches.** The most closely related approaches to our method are the ones that use pattern recognition tasks to provide guidance through visual semantic information. In contrast to such methods, our approach transcends the limitations of visual semantic information by utilizing deeper-level textual semantic information, guiding the feature extraction and selection in fusion tasks through language and textual features. The integration of VLM in image fusion tasks promises a transformative shift, enabling a more holistic understanding of images through the combined perspectives of both visual perception and textual context, thereby paving the way for more sophisticated and application-specific fusion techniques.

3. Method

In this paper, we denote the input pairs of images, which may be a pair of infrared-visible, medical, multi-exposure, or multi-focus images, as I_1 and I_2 . The algorithm ultimately outputs a fused image, represented as F . In this section, we will provide a comprehensive description of our FILM algorithm, denoted as $I_F = \text{FILM}(I_1, I_2)$, elucidating its workflow and design details. The training detail, including the loss function, will also be discussed.

3.1. Problem Overview

Brief and detailed workflows of our FILM paradigm are illustrated in Figs. 1 and 2. The algorithm is segmented into three components: *text feature fusion*, *language-guided vision feature fusion*, and *vision feature decoding*, corresponding to the first, second, and third columns of Fig. 2, and denoted as $\mathcal{T}(\cdot)$, $\mathcal{V}(\cdot)$, and $\mathcal{D}(\cdot)$, respectively. Specifically, the FILM algorithm takes two source images $\{I_1, I_2\}$ as input, which are initially processed by the *text feature fusion* component \mathcal{T} . This component encompasses generating prompts from image caption, dense caption, and Segment Anything, to produce textual descriptions via ChatGPT. The captions were en-

coded via the text encoder of BLIP2 [20], and subsequently fused them. The *language-guided vision feature fusion* component \mathcal{V} then utilizes the fused text features to guide the extraction of visual features from the source images using cross-attention. This process identifies and integrates the salient aspects and advantages to be incorporated into the fused image. Finally, the fused result F is output by the *vision feature decoding* component \mathcal{D} , which decodes the fused vision features into an image. Each component’s details will be elaborated upon separately. For more detailed explanations of the network architecture, please refer to the supplementary material due to space constraints.

3.2. Fusion via Vision-Language Model

Component I: Text feature fusion. In the text feature fusion component, paired source images $\{I_1, I_2\}$ are input, resulting in the fused text feature Φ_F^T , i.e.,

$$\Phi_F^T = \mathcal{T}(I_1, I_2). \quad (1)$$

Initially, inspired by [16, 20, 35, 75], we input the images into the BLIP2 [20], GRIT [35], and Segment Anything [16] models to extract image semantic information from holistic to fine-grained, as *Image Caption*, *Dense Caption*, and *Semantic Mask*. Subsequently, these three prompts are fed into the ChatGPT model to generate paired text descriptions $\{T_1, T_2\}$ for the source images $\{I_1, I_2\}$. We then input $\{T_1, T_2\}$ into the text encoder of parameter-frozen BLIP2 [20] model, obtaining the corresponding text features $\{\Phi_1^T, \Phi_2^T\}$. Ultimately, the fused text feature Φ_F^T is obtained by concatenating $\{\Phi_1^T, \Phi_2^T\}$. For more details on feature prompting and text generation, please refer to Sec. 4.

Component II: Language-guided vision feature fusion. In the language-guided vision feature fusion component, we guide the extraction of visual features from the source image through text features, resulting in the visual fusion feature Φ_F^V , i.e.

$$\Phi_F^V = \mathcal{V}(\Phi_F^T, I_1, I_2) \quad (2)$$

Firstly, source images $\{I_1, I_2\}$ are fed into the image encoders, producing shallow visual features $\{\Phi_1^{V,(0)}, \Phi_2^{V,(0)}\}$. The image encoder, consisting of Restormer blocks [67] and CNNs, focuses on both global and local visual representations while maintaining computational efficiency and effective feature extraction. Subsequently, these shallow features are input into the cross-attention mechanism, where fused text features guide the visual feature extraction paying more attention to the aspects of the source image desired to be preserved in the fused image. That is:

$$\Phi_1^{V,(m)} = \mathcal{CA} \left(\Phi_F^T, \Phi_1^{V,(m-1)} \right), \quad (3)$$

where $m = 1, \dots, M$. $\mathcal{CA}(\cdot)$ represents the Cross-Attention module, and $\Phi_2^{V,(m)}$ can be obtained similarly by replacing the subscripts. In the Cross-Attention layer, *Key* (K)

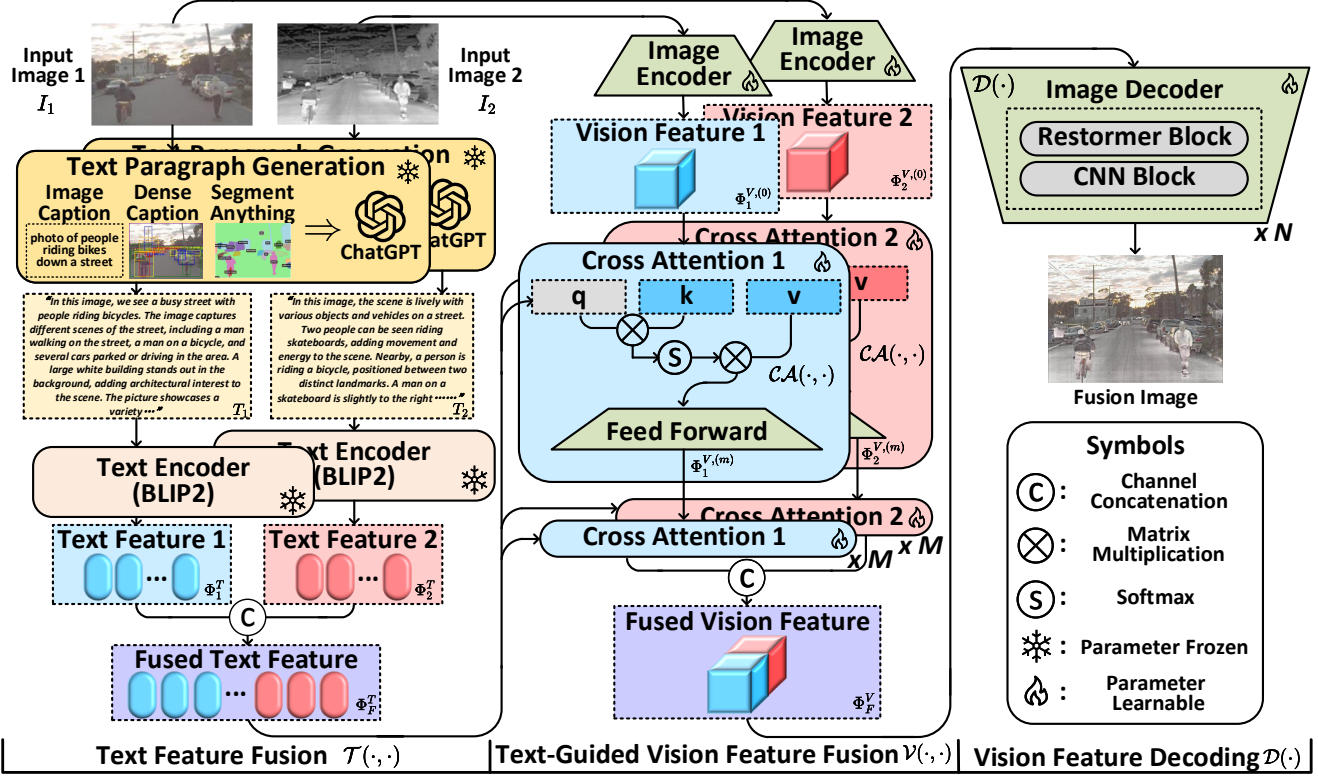


Figure 2. Workflow for our FILM, which encompasses three components: text paragraph generation and text feature fusion, language-guided vision feature fusion via cross attention and vision feature decoding, corresponding to the first, second, and third columns.

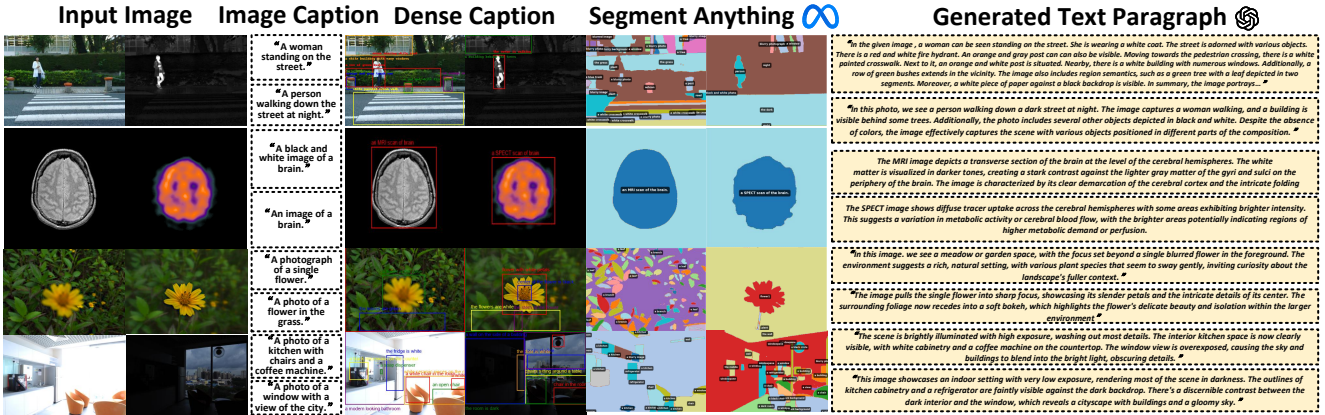


Figure 3. Visualization of the VLF dataset creation process and representative data displays.

and Value (V) are provided by $\Phi_1^{V,(m-1)}$ or $\Phi_2^{V,(m-1)}$, while Query (Q) is provided by Φ_T^T . Moreover, the feed-forward operation in the Cross-Attention Layer is also implemented through the Restormer block. After passing through M Cross-Attention layers, the text-guided visual features are represented as $\{\Phi_1^{V,(M)}, \Phi_2^{V,(M)}\}$. Subsequently, after the concatenation through channel dimension, $\{\Phi_1^{V,(M)}, \Phi_2^{V,(M)}\}$ yield the fused visual feature Φ_F^V .

Component III: Vision feature decoding. Finally, the fused visual feature is input into a decoder comprising N layers

of Restormer [67] and CNN blocks, from which the fused image is output, denoted as $I_F = \mathcal{D}(\Phi_F^V)$. I_F refers to the final output fusion image of FILM.

4. Vision-Language Fusion Datasets

In this section, we will introduce the details of the proposed *Vision-Language Fusion* (VLF) dataset, including prompt generation, paragraph descriptions output, and present representative visualizations.

Overview. Considering the high computational cost of in-



Figure 4. Visualization comparison of the fusion results in the infrared-visible image fusion task.

Table 1. Quantitative results of IVF. The red and blue markers represent the best and second-best values, respectively.

	MSRS Infrared-Visible Fusion Dataset						M ³ FD Infrared-Visible Fusion Dataset						RoadScene Infrared-Visible Fusion Dataset							
	EN	SD	SF	AG	VIF	Qabf	EN	SD	SF	AG	VIF	Qabf	EN	SD	SF	AG	VIF	Qabf		
SDN	5.25	17.35	8.67	2.67	0.50	0.38	SDN	6.85	35.19	14.65	5.29	0.57	0.54	SDN	7.30	44.20	15.13	6.03	0.59	0.52
TarD	5.28	25.22	5.98	1.83	0.42	0.18	TarD	6.76	39.13	8.19	2.97	0.53	0.30	TarD	7.27	47.24	11.40	4.29	0.54	0.42
DeF	6.46	37.63	8.60	2.80	0.77	0.54	DeF	6.90	36.22	9.61	3.51	0.61	0.43	DeF	7.34	46.50	11.38	4.53	0.59	0.48
Meta	5.65	24.97	9.99	3.40	0.63	0.48	Meta	6.66	29.01	15.88	5.74	0.69	0.56	Meta	6.89	32.03	15.35	5.95	0.53	0.45
CDDF	6.70	43.39	11.56	3.74	1.05	0.69	CDDF	7.08	41.30	16.02	5.53	0.79	0.62	CDDF	7.46	56.06	18.12	6.48	0.64	0.49
LRR	6.19	31.78	8.46	2.63	0.54	0.46	LRR	6.56	29.09	11.41	4.01	0.57	0.50	LRR	7.07	38.73	11.90	4.54	0.43	0.34
MURF	5.04	20.63	10.49	3.38	0.44	0.36	MURF	6.57	28.24	11.36	4.59	0.40	0.31	MURF	6.89	33.25	14.53	5.62	0.49	0.44
DDFM	6.19	29.26	7.44	2.51	0.73	0.48	DDFM	6.80	32.16	9.79	3.54	0.64	0.47	DDFM	7.19	41.60	11.09	4.30	0.59	0.48
SegM	5.95	37.28	11.10	3.47	0.88	0.63	SegM	6.84	34.55	15.69	5.58	0.79	0.64	SegM	7.29	46.34	14.97	5.80	0.62	0.55
FILM	6.72	43.20	11.76	3.89	1.06	0.73	FILM	7.11	41.73	16.62	5.81	0.84	0.66	FILM	7.48	53.10	19.19	7.19	0.64	0.57

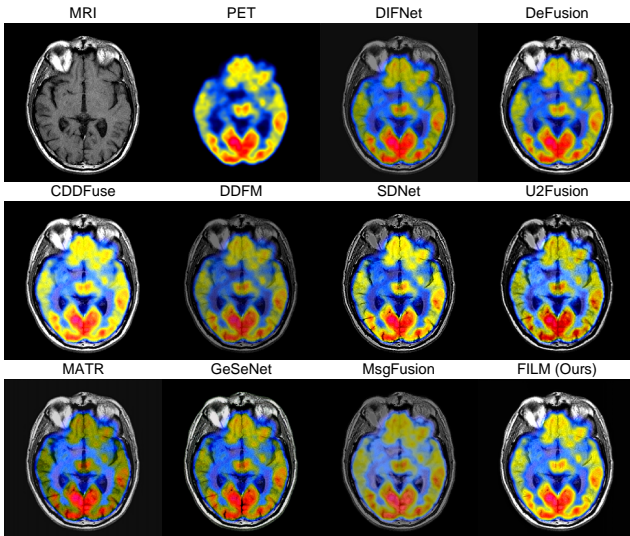


Figure 5. Visualization comparison of the fusion results in the medical image fusion task.

voicing various vision-language components, and to facilitate subsequent research on image fusion based on Vision-Language models, we propose the VLF Dataset. This dataset encompasses paired paragraph descriptions generated by ChatGPT, covering all image pairs from the training and test sets of the eight widely-used fusion datasets. These include

Table 2. Quantitative results of MIF. The red and blue markers represent the best and second-best values, respectively.

	Harvard Medical Image Fusion Dataset					
	EN	SD	SF	AG	VIF	Qabf
DIFNet	4.63	48.97	15.27	4.27	0.61	0.54
DeFusion	4.04	59.56	18.94	4.94	0.62	0.59
CDDFuse	4.12	69.23	25.13	6.39	0.72	0.69
DDFM	3.86	55.67	17.09	4.40	0.68	0.61
SDNet	3.76	51.98	24.71	6.01	0.52	0.60
U2Fusion	3.74	49.87	20.19	5.25	0.46	0.51
MATR	4.30	49.89	18.51	5.01	0.75	0.68
GeSeNet	4.46	67.12	25.47	6.55	0.76	0.76
MsgFusion	4.16	73.02	23.76	5.89	0.49	0.52
FILM	4.74	69.48	25.58	6.71	0.77	0.76

the MSRS [46], M³FD [24] and RoadScene [57] datasets for *infrared-visible image fusion (IVF)*, the Harvard dataset [14] for *medical image fusion (MIF)*, the RealMFF [69] and Lytro [34] datasets for *multi-focus image fusion (MFF)*, and the SICE [3] and MEFB [71] datasets for *multi-exposure image fusion (MEF)* tasks.

Prompt generation. The output of each component in the Text Paragraph Generation module is shown in Fig. 3. Firstly, inspired by [75], BLIP2 [20], GRIT [35] and Segment Anything [16] models output Image Caption, Dense Caption, and Semantic Mask, respectively. They provide a one-sentence caption, object-level information, and semantic mask for the

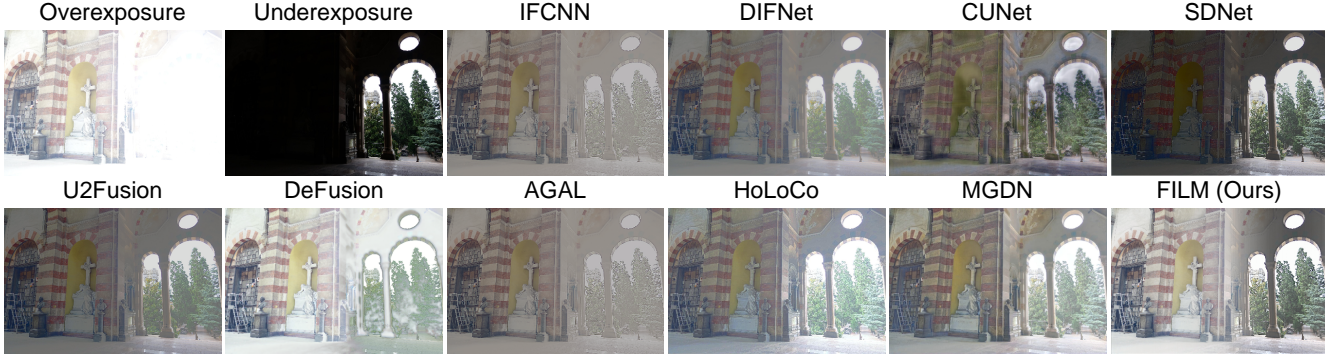


Figure 6. Visualization comparison of the fusion results in the multi-exposure image fusion task.

Table 3. Quantitative results of MEF. The red and blue markers represent the best and second-best values, respectively.

	SICE Multi-exposure Image Fusion Dataset						MEFB Multi-exposure Image Fusion Dataset						
	EN	SD	SF	AG	VIF	Qabf	EN	SD	SF	AG	VIF	Qabf	
IFCNN	6.63	39.22	16.67	4.48	0.74	0.71	IFCNN	6.99	52.49	18.16	5.34	0.71	0.69
DIFNet	6.53	35.46	11.79	3.05	0.46	0.50	DIFNet	6.99	50.23	11.79	3.47	0.51	0.53
CUNet	6.87	33.79	11.78	3.75	0.73	0.51	CUNet	7.18	45.37	12.78	4.28	0.71	0.50
SDNet	6.43	37.28	19.12	4.69	0.47	0.45	SDNet	6.59	51.77	20.53	5.27	0.55	0.42
U2Fusion	6.39	34.38	10.62	3.12	0.48	0.57	U2Fusion	6.67	46.73	12.54	3.82	0.51	0.56
DeFusion	6.86	45.00	14.21	3.97	0.89	0.57	DeFusion	7.10	56.46	14.86	4.48	0.70	0.59
AGAL	7.05	45.65	16.52	4.85	0.73	0.52	AGAL	7.14	60.63	17.77	5.33	0.79	0.65
HoLoCo	7.02	42.34	9.09	3.40	0.75	0.36	HoLoCo	7.20	53.88	12.80	4.34	0.73	0.54
MGDN	6.89	42.73	14.88	4.51	0.87	0.64	MGDN	7.25	55.97	18.09	5.76	0.96	0.65
FILM	7.07	54.99	19.46	5.10	1.07	0.79	FILM	7.37	69.35	21.08	6.19	0.99	0.76

input and representing semantic information ranging from coarse-grained to fine-grained.

Generated paragraph descriptions. Subsequently, the generated semantic prompts from paired images are input into ChatGPT [37] to generate paragraph descriptions, which are used to guide subsequent fusion tasks.

Statistical Information. This dataset contains 7040 paragraph descriptions, with each description consisting of at least seven sentences and 186 words on average. We present examples of representative multi-modality, multi-exposure, multi-focus image pairs in Fig. 3. More dataset details can be found in the supplementary materials.

5. Experiment

In this section, we will demonstrate the performance of the FILM on various fusion tasks, showcasing its superiority. Due to space constraints, more dataset introductions, hyperparameter selections and visual results are presented in the supplementary materials.

Loss function. For the total training loss, we set it as:

$$\mathcal{L}_{total} = \mathcal{L}_{int} + \alpha_1 \mathcal{L}_{grad} + \alpha_2 \mathcal{L}_{SSIM}, \quad (4)$$

where α_1, α_2 are tuning parameters. In IVF task, following

the setting in [80], $\mathcal{L}_{int} = \frac{1}{HW} \|I_F - \max(I_1, I_2)\|_1$, and $\mathcal{L}_{grad} = \frac{1}{HW} \| |\nabla I_F| - \max(|\nabla I_1|, |\nabla I_2|) \|_1$. ∇ indicates the Sobel gradient operator. α_1 and α_2 are set to 10 and 0, respectively. MIF task does not need fine-tuning training, therefore it has no loss function. For MFF and MEF tasks, inspired by [27], we set $\mathcal{L}_{int} = \frac{1}{HW} \|I_F - \text{mean}(I_1, I_2)\|_1$, $\mathcal{L}_{grad} = \frac{1}{HW} \| |\nabla I_F| - \max(|\nabla I_1|, |\nabla I_2|) \|_1$ and $\mathcal{L}_{SSIM} = 1 - \text{MEFSSIM}(I_F, I_1, I_2)$. $\{\alpha_1, \alpha_2\}$ are set to $\{50, 10\}$ and $\{100, 1\}$ in MFF and MEF tasks, respectively, in order to ensure the magnitude comparable in each term.

Training details. A machine with eight NVIDIA GeForce RTX 3090 GPUs is utilized for our experiments. We train the network for 300 epochs using the Adam optimizer, with an initial learning rate of $1e-4$ and decreasing by a factor of 0.5 every 50 epochs. The Adam optimization method is employed with the batchsize set as 16. We incorporate Restormer blocks [67] in both language-guided vision encoder $\mathcal{V}(\cdot)$ and vision feature decoder $\mathcal{D}(\cdot)$, with each block having 8 attention heads and a dimensionality of 64. M and N , representing the number of blocks in $\mathcal{V}(\cdot)$ and $\mathcal{D}(\cdot)$, are set to 2 and 3, respectively.

Metrics. We employ six quantitative metrics to assess the fusion outcomes: entropy (EN), standard deviation (SD), spatial frequency (SF), average gradient (AG), visual infor-

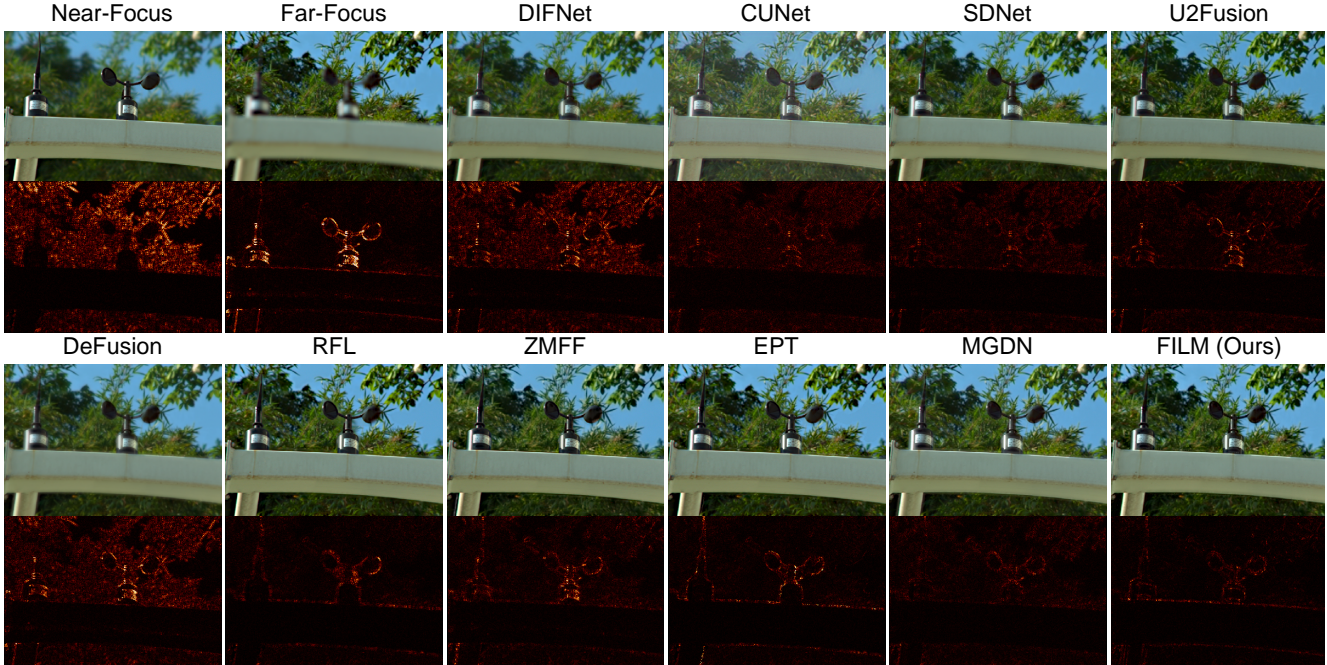


Figure 7. Visualization comparison of the fusion results and error maps in the multi-focus image fusion task.

Table 4. Quantitative results of MFF. The red and blue markers represent the best and second-best values, respectively.

	RealMFF Multi-focus Image Fusion Dataset						Lytro Multi-focus Image Fusion on Dataset						
	EN	SD	SF	AG	VIF	Qabf	EN	SD	SF	AG	VIF	Qabf	
DIFNet	7.01	51.17	10.78	3.96	0.89	0.69	DIFNet	7.43	52.52	11.47	4.30	0.73	0.54
CUNet	6.72	38.97	13.59	4.81	0.77	0.65	CUNet	7.25	45.78	15.54	5.58	0.71	0.65
SDNet	6.95	50.96	15.22	5.02	0.93	0.73	SDNet	7.47	55.25	16.88	5.84	0.84	0.69
U2Fusion	6.77	48.49	14.07	5.09	0.95	0.70	U2Fusion	7.30	51.95	14.83	5.60	0.83	0.65
DeFusion	7.09	54.42	11.24	4.08	0.98	0.69	DeFusion	7.52	56.65	11.55	4.35	0.80	0.55
RFL	7.00	51.62	14.93	5.03	0.96	0.75	RFL	7.53	57.53	19.43	6.84	0.94	0.73
ZMFF	6.99	51.15	13.93	4.95	0.94	0.70	ZMFF	7.53	56.96	18.84	6.76	0.93	0.69
EPT	7.00	51.64	14.97	5.04	0.96	0.75	EPT	7.53	57.55	19.44	6.84	0.94	0.74
MGDN	7.09	54.24	15.15	5.24	1.07	0.75	MGDN	7.54	57.50	18.81	6.67	0.93	0.74
FILM	7.11	54.62	15.65	5.41	1.09	0.76	FILM	7.55	58.60	19.51	6.97	0.97	0.74

mation fidelity (VIF), $Q^{AB/F}$. Higher metric values indicate superior quality in the fused image. Further information is available in [30].

5.1. Infrared and Visible Image Fusion

Setup. Following [80, 82], infrared-visible fusion experiments are conducted on the MSRS [46], M³FD [24] and RoadScene [57] datasets. 1083 image pairs in MSRS are for training and 361 pairs are for testing. The generalizability of FILM is further assessed by M³FD and RoadScene without finetuning. We evaluated FILM against various state-of-the-art (SOTA) methods including SDNet [68], TarDAL [24], DeFusion [23], MetaFusion [76], CDDFuse [80], LRRNet

[18], MURF [61], DDFM [82], and SegMIF [26].

Comparison with SOTA methods. In Fig. 4, FILM successfully integrated the thermal radiation information with the detailed texture features. Leveraging textual features and knowledge, the fusion process enhanced the visibility of objects in low-light environments, making textures and contours clearer, and reducing artifacts. For the quantitative results in Tab. 1, our method showcases exceptional performance in almost all metrics, confirming its adaptability for various environmental scenarios and object categories. Hence, FILM is proven to well maintain the completeness and richness of the information from source images, and generate results that conform to human visual perception.

Ablation studies. To explore the effectiveness of each mod-

Table 5. Ablation experiments results, with red resent best values.

	IC	DC	SM	GPT	EN	SD	SF	AG	VIF	Qabf
I: w/o text					7.16	43.45	11.58	5.63	0.51	0.48
II: w/o caption				✓	7.25	45.66	11.94	5.99	0.54	0.51
III: w/o DC and SM	✓			✓	7.26	47.71	11.87	6.05	0.55	0.53
IV: w/o SM	✓	✓		✓	7.33	49.09	16.36	6.94	0.62	0.55
V: w/o GPT	✓	✓	✓		7.29	50.38	14.39	6.55	0.58	0.53
ours	✓	✓	✓	✓	7.48	53.10	19.19	7.19	0.64	0.57

ule in our proposed method, we conduct ablation studies on the test dataset of RoadScene [57], whose results are presented in Tab. 5. In Exp. I, we remove the guidance through textual information and only use image features for fusion, i.e., the cross-attention layers between text and image features are eliminated, aiming to demonstrate the effect of text-guided feature extraction and fusion in FILM. By increasing the number of Restormer blocks, we maintain the total number of parameters close to the original model. Then, in Exp. II-IV, we test the guiding role of text semantic prompts from holistic to fine-grained, including image caption (IC), dense caption (DC), and segment mask (SM). In Exp. II, we directly feed the source images into ChatGPT. By manually providing prompts, GPT generates overall descriptions of the images, which are used as text inputs for image fusion. This study bypassed the steps involving prompts from IC, DC and SM. In Exp. III, only IC is input into GPT, whereas in Exp. IV, both IC and DC are together input into GPT, revealing the importance of different aspects of the captions from coarse-grained to fine-grained. Finally, in Exp. V, after extracting IC, DC and SM from images, we directly concatenate these three captions as the text description without inputting them into GPT. This is to demonstrate GPT’s capability in integrating textual information and its effort for fusion performance. In conclusion, ablation experiments demonstrate that by relying on the comprehensive information from different grains of captions and the powerful summarization capability of GPT, our experimental setup achieved optimal fusion performance, validating the rationality of FILM setting.

5.2. Medical Image Fusion

Setup. Following [82], we engage the Harvard Medical dataset [14], which consisted of 50 pairs of MRI-CT, MRI-PET, and MRI-SPECT images, to evaluate the generalizability of our model. Notably, we employ the model trained on the IVF experiments and conducted a generalization test on the Harvard Medical dataset without any fine-tuning. The competitors include DIF-Net [15], SDNet [68], U2Fusion [59], DeFusion [23], MATR [47], CDDFuse [80], DDFM [81], GeSeNet [22], MsgFusion [53]. Results from DIF-Net, DeFusion, CDDFuse and DDFM are the generalized outcomes of IVF models without fine-tuning, whereas the other results are from models specialized training using the MIF

datasets.

Comparison with SOTA methods. In terms of visual perception and quantitative analysis (Fig. 5 and Tab. 2), FILM has shown outstanding accuracy in extracting cross-modal structural highlights and detailed texture features, effectively integrating source information into the fused images. These achievements surpass even those of fusion models specifically fine-tuned via medical image pairs.

5.3. Multi-exposure Image Fusion

Setup. We conduct MEF experiments on the SICE [3] and MEFB [71] dataset. We utilized 499 pairs from SICE dataset for training, while 90 pairs from SICE and 40 pairs from MEFB for testing. Our comparison methods encompass IFCNN [74], DIFNet [15], CUNet [4], SDNet [68], U2Fusion [59], DeFusion [23], AGAL [25], HoLoCo [27] and MGDN [7].

Comparison with SOTA methods. Both quantitative and qualitative results in Tab. 3 and Fig. 6 demonstrate the effectiveness of FILM, which adeptly handles multiple images with varying exposures, expanding the dynamic range while simultaneously improving image quality and enhancing contrast.

5.4. Multi-focus Image Fusion

Setup. MFF experiments are conducted using RealMFF [69] and Lytro [34]. 639 image pairs from RealMFF are employed for training, while 71 pairs from it are reserved for testing and 20 image pairs in Lytro are utilized for generalizability test. Comparative methods encompass DIFNet [15], CUNet [4], SDNet [68], U2Fusion [59], DeFusion [23], RFL [51], ZMFF [11], EPT [52], and MGDN [7].

Comparison with SOTA methods. As illustrated in Fig. 7, benefiting from textual descriptions, FILM excels in identifying clear regions within multi-focus image pairs, ensuring sharp foreground and background elements. The quantitative results in Tab. 4 further underscore the excellence of our methodology.

6. Conclusion

This work addresses a critical limitation of existing image fusion techniques: their insufficient exploitation of deeper semantic information beyond visual features. To this end, we present, for the first time, a novel paradigm called Image Fusion via Vision-Language Model (FILM), which leverages explicit textural descriptions of source images from large language models to guide the fusion process, enabling a more comprehensive understanding of image content. FILM demonstrates promising results on various image fusion tasks, including infrared visible, medical, multi-exposure and multi-focus scenarios. In addition, we present a novel benchmark vision language dataset, including ChatGPT-based descriptions for eight image fusion datasets. We hope

that our study will open up new opportunities for large-scale vision-language models in the realm of image fusion.

References

- [1] Odysseas Bouzos, Ioannis Andreadis, and Nikolaos Mitanoudis. A convolutional neural network-based conditional random field model for structured multi-focus image fusion robust to noise. *IEEE Transactions on Image Processing*, 2023. 2
- [2] Tim Brooks, Aleksander Holynski, and Alexei A Efros. Instructpix2pix: Learning to follow image editing instructions. In *Proceedings of the IEEE/CVF Conference on Computer Vision and Pattern Recognition*, pages 18392–18402, 2023. 2
- [3] Jianrui Cai, Shuhang Gu, and Lei Zhang. Learning a deep single image contrast enhancer from multi-exposure images. *IEEE Transactions on Image Processing*, 27(4):2049–2062, 2018. 2, 5, 8
- [4] Xin Deng and Pier Luigi Dragotti. Deep convolutional neural network for multi-modal image restoration and fusion. *IEEE Transactions on Pattern Analysis and Machine Intelligence*, 43(10):3333–3348, 2021. 1, 2, 8
- [5] Xin Deng, Yutong Zhang, Mai Xu, Shuhang Gu, and Yiping Duan. Deep coupled feedback network for joint exposure fusion and image super-resolution. *IEEE Transactions on Image Processing*, 30:3098–3112, 2021. 2
- [6] Fangyuan Gao, Xin Deng, Mai Xu, Jingyi Xu, and Pier Luigi Dragotti. Multi-modal convolutional dictionary learning. *IEEE Transactions on Image Processing*, 31:1325–1339, 2022. 2
- [7] Yuanshen Guan, Ruikang Xu, Mingde Yao, Lizhi Wang, and Zhiwei Xiong. Mutual-guided dynamic network for image fusion. In *ACM Multimedia*, pages 1779–1788. ACM, 2023. 8
- [8] Yuanshen Guan, Ruikang Xu, Mingde Yao, Lizhi Wang, and Zhiwei Xiong. Mutual-guided dynamic network for image fusion. In *Proceedings of the 31st ACM International Conference on Multimedia*, pages 1779–1788, 2023. 2
- [9] Xiaopeng Guo, Rencan Nie, Jinde Cao, Dongming Zhou, Liye Mei, and Kangjian He. Fusegan: Learning to fuse multi-focus image via conditional generative adversarial network. *IEEE Trans. Multimedia*, 21(8):1982–1996, 2019. 2
- [10] Dong Han, Liang Li, Xiaojie Guo, and Jiayi Ma. Multi-exposure image fusion via deep perceptual enhancement. *Information Fusion*, 79:248–262, 2022. 2
- [11] Xingyu Hu, Junjun Jiang, Xianming Liu, and Jiayi Ma. Zmff: Zero-shot multi-focus image fusion. *Information Fusion*, 92:127–138, 2023. 8
- [12] Alex Pappachen James and Belur V. Dasarathy. Medical image fusion: A survey of the state of the art. *Information Fusion*, 19:4–19, 2014. 1
- [13] Zhiying Jiang, Zengxi Zhang, Xin Fan, and Risheng Liu. Towards all weather and unobstructed multi-spectral image stitching: Algorithm and benchmark. In *Proceedings of the ACM International Conference on Multimedia (ACM MM)*, pages 3783–3791, 2022. 2
- [14] BKeith A. Johnson and J. Alex Becker. Harvard medical website. <http://www.med.harvard.edu/AANLIB/home.html>. 5, 8
- [15] Hyungjoo Jung, Youngjung Kim, Hyunsung Jang, Namkoo Ha, and Kwanghoon Sohn. Unsupervised deep image fusion with structure tensor representations. *IEEE Transactions on Image Processing*, 29:3845–3858, 2020. 8
- [16] Alexander Kirillov, Eric Mintun, Nikhila Ravi, Hanzi Mao, Chloe Rolland, Laura Gustafson, Tete Xiao, Spencer Whitehead, Alexander C. Berg, Wan-Yen Lo, Piotr Dollar, and Ross Girshick. Segment anything. In *Proceedings of the IEEE/CVF International Conference on Computer Vision (ICCV)*, pages 4015–4026, 2023. 3, 5
- [17] Hui Li and Xiao-Jun Wu. Densefuse: A fusion approach to infrared and visible images. *IEEE Transactions on Image Processing*, 28(5):2614–2623, 2018. 2
- [18] Hui Li, Tianyang Xu, Xiaojun Wu, Jiwen Lu, and Josef Kittler. Lrnet: A novel representation learning guided fusion network for infrared and visible images. *IEEE Transactions on Pattern Analysis and Machine Intelligence*, 45(9):11040–11052, 2023. 2, 7
- [19] Junnan Li, Dongxu Li, Caiming Xiong, and Steven C. H. Hoi. BLIP: bootstrapping language-image pre-training for unified vision-language understanding and generation. In *ICML*, pages 12888–12900. PMLR, 2022. 2, 3
- [20] Junnan Li, Dongxu Li, Silvio Savarese, and Steven C. H. Hoi. BLIP-2: bootstrapping language-image pre-training with frozen image encoders and large language models. In *ICML*, pages 19730–19742. PMLR, 2023. 1, 3, 5
- [21] Jiawei Li, Jinyuan Liu, Shihua Zhou, Qiang Zhang, and Nikola K. Kasabov. Gesenet: A general semantic-guided network with couple mask ensemble for medical image fusion. *IEEE Transactions on Neural Networks and Learning Systems*, pages 1–14, 2023. 1
- [22] Jiawei Li, Jinyuan Liu, Shihua Zhou, Qiang Zhang, and Nikola K Kasabov. Gesenet: A general semantic-guided network with couple mask ensemble for medical image fusion. *IEEE Transactions on Neural Networks and Learning Systems*, 2023. 8
- [23] Pengwei Liang, Junjun Jiang, Xianming Liu, and Jiayi Ma. Fusion from decomposition: A self-supervised decomposition approach for image fusion. In *Proceedings of the European Conference on Computer Vision (ECCV)*, pages 719–735, 2022. 1, 2, 7, 8
- [24] Jinyuan Liu, Xin Fan, Zhanbo Huang, Guanyao Wu, Risheng Liu, Wei Zhong, and Zhongxuan Luo. Target-aware dual adversarial learning and a multi-scenario multi-modality benchmark to fuse infrared and visible for object detection. In *Proceedings of the IEEE/CVF Conference on Computer Vision and Pattern Recognition (CVPR)*, pages 5792–5801, 2022. 1, 2, 5, 7
- [25] Jinyuan Liu, Jingjie Shang, Risheng Liu, and Xin Fan. Attention-guided global-local adversarial learning for detail-preserving multi-exposure image fusion. *IEEE Transactions on Circuits and Systems for Video Technology*, 32(8):5026–5040, 2022. 8
- [26] Jinyuan Liu, Zhu Liu, Guanyao Wu, Long Ma, Risheng Liu, Wei Zhong, Zhongxuan Luo, and Xin Fan. Multi-interactive

- feature learning and a full-time multi-modality benchmark for image fusion and segmentation. In *Proceedings of the IEEE/CVF International Conference on Computer Vision (ICCV)*, pages 8115–8124, 2023. 2, 7
- [27] Jinyuan Liu, Guanyao Wu, Junsheng Luan, Zhiying Jiang, Risheng Liu, and Xin Fan. Holoco: Holistic and local contrastive learning network for multi-exposure image fusion. *Information Fusion*, 95:237–249, 2023. 2, 6, 8
- [28] Yu Liu, Xun Chen, Hu Peng, and Zengfu Wang. Multi-focus image fusion with a deep convolutional neural network. *Information Fusion*, 36:191–207, 2017. 2
- [29] Haoyu Ma, Qingmin Liao, Juncheng Zhang, Shaojun Liu, and Jing-Hao Xue. An α -matte boundary defocus model-based cascaded network for multi-focus image fusion. *IEEE Transactions on Image Processing*, 29:8668–8679, 2020. 2
- [30] Jiayi Ma, Yong Ma, and Chang Li. Infrared and visible image fusion methods and applications: A survey. *Information Fusion*, 45:153–178, 2019. 7
- [31] Jiayi Ma, Wei Yu, Pengwei Liang, Chang Li, and Junjun Jiang. FusionGAN: A generative adversarial network for infrared and visible image fusion. *Information Fusion*, 48:11–26, 2019. 2
- [32] Kede Ma, Hui Li, Hongwei Yong, Zhou Wang, Deyu Meng, and Lei Zhang. Robust multi-exposure image fusion: A structural patch decomposition approach. *IEEE Transactions on Image Processing*, 26(5):2519–2532, 2017. 1
- [33] Kede Ma, Zhengfang Duanmu, Hanwei Zhu, Yuming Fang, and Zhou Wang. Deep guided learning for fast multi-exposure image fusion. *IEEE Transactions on Image Processing*, 2020. 1
- [34] Mansour Nejati, Shadrokh Samavi, and Shahram Shirani. Multi-focus image fusion using dictionary-based sparse representation. *Information Fusion*, 25:72–84, 2015. 5, 8
- [35] Van-Quang Nguyen, Masanori Suganuma, and Takayuki Okatani. Grit: Faster and better image captioning transformer using dual visual features. In *European Conference on Computer Vision*, pages 167–184. Springer, 2022. 3, 5
- [36] OpenAI. Gpt-4 technical report. *ArXiv*, abs/2303.08774, 2023. 2, 3
- [37] OpenAI. *ChatGPT*, 2023. 2, 6
- [38] K Ram Prabhakar, V Sai Srikar, and R Venkatesh Babu. Deepfuse: A deep unsupervised approach for exposure fusion with extreme exposure image pairs. In *Proceedings of the IEEE International Conference on Computer Vision (ICCV)*, pages 4724–4732, 2017. 2
- [39] Linhao Qu, Shaolei Liu, Manning Wang, and Zhijian Song. Transmef: A transformer-based multi-exposure image fusion framework using self-supervised multi-task learning. In *Proceedings of the AAAI conference on artificial intelligence*, pages 2126–2134, 2022. 2
- [40] Alec Radford, Jong Wook Kim, Chris Hallacy, Aditya Ramesh, Gabriel Goh, Sandhini Agarwal, Girish Sastry, Amanda Askell, Pamela Mishkin, Jack Clark, et al. Learning transferable visual models from natural language supervision. In *International conference on machine learning*, pages 8748–8763. PMLR, 2021. 2
- [41] Aditya Ramesh, Mikhail Pavlov, Gabriel Goh, Scott Gray, Chelsea Voss, Alec Radford, Mark Chen, and Ilya Sutskever. Zero-shot text-to-image generation. In *International Conference on Machine Learning*, pages 8821–8831. PMLR, 2021. 3
- [42] Aditya Ramesh, Prafulla Dhariwal, Alex Nichol, Casey Chu, and Mark Chen. Hierarchical text-conditional image generation with clip latents. *arXiv preprint arXiv:2204.06125*, 1(2): 3, 2022. 3
- [43] Yiming Sun, Bing Cao, Pengfei Zhu, and Qinghua Hu. Det-fusion: A detection-driven infrared and visible image fusion network. In *Proceedings of the ACM International Conference on Multimedia (ACM MM)*, pages 4003–4011, 2022. 2
- [44] Linfeng Tang, Yuxin Deng, Yong Ma, Jun Huang, and Jiayi Ma. Superfusion: A versatile image registration and fusion network with semantic awareness. *IEEE/CAA Journal of Automatica Sinica*, 9(12):2121–2137, 2022. 2
- [45] Linfeng Tang, Jiteng Yuan, and Jiayi Ma. Image fusion in the loop of high-level vision tasks: A semantic-aware real-time infrared and visible image fusion network. *Information Fusion*, 82:28–42, 2022. 2
- [46] Linfeng Tang, Jiteng Yuan, Hao Zhang, Xingyu Jiang, and Jiayi Ma. Piafusion: A progressive infrared and visible image fusion network based on illumination aware. *Information Fusion*, 83-84:79–92, 2022. 5, 7
- [47] Wei Tang, Fazhi He, Yu Liu, and Yansong Duan. Matr: Multimodal medical image fusion via multiscale adaptive transformer. *IEEE Transactions on Image Processing*, 31: 5134–5149, 2022. 8
- [48] Hugo Touvron, Thibaut Lavril, Gautier Izacard, Xavier Martinet, Marie-Anne Lachaux, Timothée Lacroix, Baptiste Rozière, Naman Goyal, Eric Hambro, Faisal Azhar, et al. Llama: Open and efficient foundation language models. *arXiv preprint arXiv:2302.13971*, 2023. 3
- [49] Di Wang, Jinyuan Liu, Xin Fan, and Risheng Liu. Unsupervised misaligned infrared and visible image fusion via cross-modality image generation and registration. In *Proceedings of the International Joint Conferences on Artificial Intelligence (IJCAI)*, pages 3508–3515, 2022. 2
- [50] Zirui Wang, Jiahui Yu, Adams Wei Yu, Zihang Dai, Yulia Tsvetkov, and Yuan Cao. Simvlm: Simple visual language model pretraining with weak supervision. *arXiv preprint arXiv:2108.10904*, 2021. 3
- [51] Zeyu Wang, Xiongfei Li, Haoran Duan, and Xiaoli Zhang. A self-supervised residual feature learning model for multifocus image fusion. *IEEE Transactions on Image Processing*, 31: 4527–4542, 2022. 2, 8
- [52] Zeyu Wang, Xiongfei Li, Libo Zhao, Haoran Duan, Shidong Wang, Hao Liu, and Xiaoli Zhang. When multi-focus image fusion networks meet traditional edge-preservation technology. *International Journal of Computer Vision*, pages 1–24, 2023. 2, 8
- [53] Jinyu Wen, Feiwei Qin, Jiao Du, Meie Fang, Xinhua Wei, CL Philip Chen, and Ping Li. Msgfusion: Medical semantic guided two-branch network for multimodal brain image fusion. *IEEE Transactions on Multimedia*, 2023. 8
- [54] Bin Xiao, Bocheng Xu, Xiuli Bi, and Weisheng Li. Global-feature encoding u-net (geu-net) for multi-focus image fusion.

- IEEE Transactions on Image Processing*, 30:163–175, 2020. 2
- [55] Bin Xiao, Haifeng Wu, and Xiuli Bi. Dtmnet: a discrete tchebichef moments-based deep neural network for multi-focus image fusion. In *Proceedings of the IEEE/CVF International Conference on Computer Vision*, pages 43–51, 2021. 2
- [56] Han Xu and Jiayi Ma. Emfusion: An unsupervised enhanced medical image fusion network. *Information Fusion*, 76:177–186, 2021. 1
- [57] Han Xu, Jiayi Ma, Zhuliang Le, Junjun Jiang, and Xiaojie Guo. FusionDn: A unified densely connected network for image fusion. In *Proceedings of the AAAI Conference on Artificial Intelligence (AAAI)*, pages 12484–12491, 2020. 5, 7, 8
- [58] Han Xu, Jiayi Ma, and Xiao-Ping Zhang. Mef-gan: Multi-exposure image fusion via generative adversarial networks. *IEEE Transactions on Image Processing*, 29:7203–7216, 2020. 2
- [59] Han Xu, Jiayi Ma, Junjun Jiang, Xiaojie Guo, and Haibin Ling. U2fusion: A unified unsupervised image fusion network. *IEEE Transactions on Pattern Analysis and Machine Intelligence*, 44(1):502–518, 2022. 2, 8
- [60] Han Xu, Jiayi Ma, Jiteng Yuan, Zhuliang Le, and Wei Liu. Rfnet: Unsupervised network for mutually reinforcing multi-modal image registration and fusion. In *Proceedings of the IEEE/CVF Conference on Computer Vision and Pattern Recognition (CVPR)*, pages 19647–19656, 2022. 2
- [61] Han Xu, Jiteng Yuan, and Jiayi Ma. MURF: mutually reinforcing multi-modal image registration and fusion. *IEEE Transactions on Pattern Analysis and Machine Intelligence*, 45(10):12148–12166, 2023. 7
- [62] Kelvin Xu, Jimmy Ba, Ryan Kiros, Kyunghyun Cho, Aaron Courville, Ruslan Salakhudinov, Rich Zemel, and Yoshua Bengio. Show, attend and tell: Neural image caption generation with visual attention. In *International conference on machine learning*, pages 2048–2057. PMLR, 2015. 2
- [63] Shuang Xu, Lizhen Ji, Zhe Wang, Pengfei Li, Kai Sun, Chunxia Zhang, and Jianshe Zhang. Towards reducing severe defocus spread effects for multi-focus image fusion via an optimization based strategy. *IEEE Transactions on Computational Imaging*, 6:1561–1570, 2020. 2
- [64] Shuang Xu, Jianshe Zhang, Zixiang Zhao, Kai Sun, Junmin Liu, and Chunxia Zhang. Deep gradient projection networks for pan-sharpening. In *Proceedings of the IEEE/CVF Conference on Computer Vision and Pattern Recognition (CVPR)*, pages 1366–1375, 2021. 2
- [65] Jia-Li Yin, Bo-Hao Chen, and Yan-Tsung Peng. Two exposure fusion using prior-aware generative adversarial network. *IEEE Transactions on Multimedia*, 24:2841–2851, 2021. 2
- [66] Jia-Li Yin, Bo-Hao Chen, Yan-Tsung Peng, and Hau Hwang. Automatic intermediate generation with deep reinforcement learning for robust two-exposure image fusion. *IEEE Transactions on Neural Networks and Learning Systems*, 33(12):7853–7862, 2021. 2
- [67] Syed Waqas Zamir, Aditya Arora, Salman Khan, Munawar Hayat, Fahad Shahbaz Khan, and Ming-Hsuan Yang. Restormer: Efficient transformer for high-resolution image restoration. In *Proceedings of the IEEE/CVF Conference on Computer Vision and Pattern Recognition (CVPR)*, pages 5718–5729, 2022. 3, 4, 6
- [68] Hao Zhang and Jiayi Ma. Sdnet: A versatile squeeze-and-decomposition network for real-time image fusion. *International Journal of Computer Vision*, 129(10):2761–2785, 2021. 7, 8
- [69] Juncheng Zhang, Qingmin Liao, Shaojun Liu, Haoyu Ma, Wenming Yang, and Jing-Hao Xue. Real-mff: A large realistic multi-focus image dataset with ground truth. *Pattern Recognition Letters*, 138:370–377, 2020. 5, 8
- [70] Shilong Zhang, Peize Sun, Shoufa Chen, Min Xiao, Wenqi Shao, Wenwei Zhang, Kai Chen, and Ping Luo. Gpt4roi: Instruction tuning large language model on region-of-interest. *arXiv preprint arXiv:2307.03601*, 2023. 2, 3
- [71] Xingchen Zhang. Benchmarking and comparing multi-exposure image fusion algorithms. *Information Fusion*, 74:111–131, 2021. 5, 8
- [72] Xingchen Zhang. Deep learning-based multi-focus image fusion: A survey and a comparative study. *IEEE Transactions on Pattern Analysis and Machine Intelligence*, 44(9):4819–4838, 2021. 1, 2
- [73] Xingchen Zhang and Yiannis Demiris. Visible and infrared image fusion using deep learning. *IEEE Transactions on Pattern Analysis and Machine Intelligence*, 45(8):10535–10554, 2023. 2
- [74] Yu Zhang, Yu Liu, Peng Sun, Han Yan, Xiaolin Zhao, and Li Zhang. IFCNN: A general image fusion framework based on convolutional neural network. *Information Fusion*, 54:99–118, 2020. 8
- [75] Hengyuan Zhao. Image.txt: Transform image into unique paragraph. <https://zhaohengyuan1.github.io/image2paragraph.github.io/>, 2023. 3, 5
- [76] Wenda Zhao, Shigeng Xie, Fan Zhao, You He, and Huchuan Lu. Metafusion: Infrared and visible image fusion via meta-feature embedding from object detection. In *CVPR*, pages 13955–13965. IEEE, 2023. 2, 7
- [77] Zixiang Zhao, Shuang Xu, Chunxia Zhang, Junmin Liu, Jianshe Zhang, and Pengfei Li. DIDFuse: Deep image decomposition for infrared and visible image fusion. In *Proceedings of the International Joint Conference on Artificial Intelligence (IJCAI)*, pages 970–976, 2020. 2
- [78] Zixiang Zhao, Shuang Xu, Jianshe Zhang, Chengyang Liang, Chunxia Zhang, and Junmin Liu. Efficient and model-based infrared and visible image fusion via algorithm unrolling. *IEEE Transactions on Circuits and Systems for Video Technology*, 32(3):1186–1196, 2022. 2
- [79] Zixiang Zhao, Jianshe Zhang, Shuang Xu, Zudi Lin, and Hanspeter Pfister. Discrete cosine transform network for guided depth map super-resolution. In *Proceedings of the IEEE/CVF Conference on Computer Vision and Pattern Recognition (CVPR)*, pages 5687–5697, 2022. 2
- [80] Zixiang Zhao, Haowen Bai, Jianshe Zhang, Yulun Zhang, Shuang Xu, Zudi Lin, Radu Timofte, and Luc Van Gool. Cddfuse: Correlation-driven dual-branch feature decomposition for multi-modality image fusion. In *Proceedings of*

the IEEE/CVF Conference on Computer Vision and Pattern Recognition (CVPR), pages 5906–5916, 2023. [1](#), [2](#), [6](#), [7](#), [8](#)

- [81] Zixiang Zhao, Haowen Bai, Yuanzhi Zhu, Jianshe Zhang, Shuang Xu, Yulun Zhang, Kai Zhang, Deyu Meng, Radu Timofte, and Luc Van Gool. DDFM: denoising diffusion model for multi-modality image fusion. *arXiv preprint arXiv:2303.06840*, 2023. [8](#)
- [82] Zixiang Zhao, Haowen Bai, Yuanzhi Zhu, Jianshe Zhang, Shuang Xu, Yulun Zhang, Kai Zhang, Deyu Meng, Radu Timofte, and Luc Van Gool. Ddfm: Denoising diffusion model for multi-modality image fusion. In *Proceedings of the IEEE/CVF International Conference on Computer Vision (ICCV)*, pages 8082–8093, 2023. [1](#), [2](#), [7](#), [8](#)
- [83] Deyao Zhu, Jun Chen, Xiaoqian Shen, Xiang Li, and Mohamed Elhoseiny. Minigt-4: Enhancing vision-language understanding with advanced large language models. *arXiv preprint arXiv:2304.10592*, 2023. [2](#), [3](#)